CLM - R 157

CLM - R 157

UKAEA RESEARCH GROUP

Report

REACTION CROSS-SECTIONS OF RELEVANCE TO HYDROGEN PLASMAS IN ION SOURCES

A R MARTIN

CULHAM LABORATORY
Abingdon Oxfordshire
1976
Available from H. M. Stationery Office

C.18

£1.50

UDC:
539.1.02:546.11
537.534.2

CLM-R 157

REACTION CROSS-SECTION OF RELEVANCE TO HYDROGEN PLASMAS IN ION SOURCES

by

A R MARTIN

ABSTRACT:

This report presents experimental data for reactions occurring between atomic hydrogen, molecular hydrogen, H_2^+ ions, and H_3^+ ions and electrons. The information is intended to be of use in the evaluation of operating conditions in ion sources, and so the data has been limited to the energy range of 0-150 eV.

Data are not given for charge-exchange processes, or for heavy particle interactions, except in the case of H_3^+ molecular ion formation.

Some data are also given for the kinetic energy distributions of the "fast" products arising from dissociative ionisation and dissociative excitation of molecular hydrogen.

Euratom-UKAEA Association for Fusion Research
Culham Laboratory
Abingdon
Oxfordshire OX14 3DB

February 1976

SBN: 85311 044 1

1. INTRODUCTION

Data on hydrogen reaction cross-sections is of use in the evaluation of operating conditions in ion sources (Green, 1974; Green et al, 1975) and other properties of the discharge plasmas e.g. species fraction under varying conditions (Martin and Green, 1976).

Discussions on reaction cross-sections are distributed throughout the literature, but otherwise comprehensive compilations e.g. Freeman and Jones (1974) generally consider only reactions involving molecular and atomic neutral hydrogen. The compilations by Barnett et al (1964) and Kieffer and Dunn (1966) give data on a wider range of reactions, but they are not complete for the case of hydrogen, and there exists a large volume of more recent work which modifies and supplements these data.

In this report, data are given for a large number of reactions occurring between atomic hydrogen, molecular hydrogen, H_2^+ ions, H_3^+ ions and electrons. In ion source discharges ionisation is due to electron bombardment, with the electrons having energies of $\sim$ 10 - 100 eV in general. For this reason the data has been limited to the energy range of 0-150 eV, although data for higher energy electrons has usually been reported in the literature.

Data are not given for charge-exchange processes, or for heavy particle interactions, except in the case of $H_2^+ + H_2$ collisions to form the H_3^+ molecular ion.

The cross-sections given have all been determined experimentally, with the exception of ionisation of the 2P radiative state of atomic hydrogen, for which theoretical cross-sections only are available. No discussion of probable errors in the experimental measurements are given, and information on this aspect should be obtained from the

literature cited. In general, it may be remarked that reactions involving H_o and H_2 initial states are well known, but some of the reactions involving H_2^+ are less well determined. Data on the various breakup reactions of H_3^+ are still scarce. Interpretation of experimental results is complicated here by the existence of a large number of possible reaction paths which hinder the identification of specific reactions when measuring cross-sections.

Some data are also given for the kinetic energy distributions of the "fast" products arising from dissociative ionisation and dissociative excitation of molecular hydrogen. The behaviour of these particles is of interest in some aspects of the study of the discharge plasma e.g. residence time calculations of neutral atoms, and loss rates of the various species from the plasma volume.

It should be noted that the cross-sections presented in this compilation represent the experimental determinations carried out to date, and are not intended to be definitive. In many cases the data require improvement or clarification, and in some cases the data are inadequate for detailed discharge studies. The compilation is intended to provide a reference guide to the work available at present on reactions occurring in hydrogen.

2. HYDROGEN ATOM REACTIONS

2.1 Ionisation $H_o + e \rightarrow H_1^+ + 2e$

The cross-section for this reaction has been measured using crossed-beam techniques by Fite and Brackman (1958a). The ratio of the cross-sections for ionisation of the atom and for molecular hydrogen was directly determined. The absolute cross-sections were then estimated by multiplying this ratio by the molecular cross-sections measured by Tate and Smith (1932).

The cross-section is shown in Figure 1, and it can be considered to be accurately known. Values of the cross-section for energies up to 1,000 eV are given in Fite and Brackman (1958a), and the data is reproduced in Kieffer and Dunn (1966).

2.2 Ionisation from excited states

Ionisation of atomic hydrogen from its excited metastable state may become an important reaction under certain conditions in a discharge e.g. in situations where a high electron number density exists, and the population of metastable atoms is large. The radiative excited state has such a short lifetime that any ionisation from it can be neglected, but excitation to this state may play a role in determining electron energy loss factors. For completeness, the excitation and ionisation cross-sections for both states are included in the compilation.

2.2.1 Excitation to the 2P and 2S states $H_o + e \rightarrow H_o^* + e$

(a) 2P radiative state

The cross-section for excitation of the $H_o(1S)$ to the $H_o^*(2P)$ short-lived radiative state has been measured by Fite and Brackman, (1958b). Lyman - α photon detection was used to give a relative cross-section curve, and this was then normalised to fit the Born-approximation at higher electron energies. It was found to deviate from the theoretical curve at energies below $\sim$ 150 eV. The lifetime of this state is $\simeq 10^{-9}$ secs.

The cross-section is shown in Figure 2. More recent data, by Long et al (1968), is also shown, and is seen to be in good agreement.

(b) 2S metastable state

The cross-section for excitation to the $H_o^*(2S)$ metastable state has been measured by Stebbings et al (1960), again by Lyman - α detection techniques. In order to assign absolute cross-sections the ratio of the 2S to the 2P excitation cross-section was determined, and the absolute 2S cross-section was found by use of the previous results for the 2P states. The values presented by Stebbings et al (1960) must be multiplied by a correction factor of 1.5 (Lichten, 1961). The experiment measured the total cross-section for 2S production, including contributions from cascades down from higher states (produced by $1S \rightarrow nP$ states, with $n \geq 3$, followed by a radiative transition to the 2S state). The $1S \rightarrow 2S$ contribution was deduced. The lifetime of this state in the absence of perturbations is $\gtrsim 10^{-3}$ secs (Fite et al, 1959), but can be considerably shorter in the presence of e.g. an electric field.

The cross-section is shown in Figure 3, for both the cascade included and 1S-2S deduced cases.

Hils et al (1966) have also measured this cross-section. They find that the total cross-section, including contributions from cascades is in excellent agreement with the data of Stebbings et al (1960). However, they used a different method of normalisation for the data, and deduced a different curve for the $1S \rightarrow 2S$ value. This is also shown on Figure 3, where it can be seen that slightly lower values of the cross-section are found. More discussion of the reduction methods can be found in Hils et al (1966).

More recent measurements of the total production cross-section, including cascade effects, have been presented by Cox and Smith (1971). The cross-section had a similar behaviour, and the data were in

reasonable agreement at energies greater than $\sim$ 100 eV. However, at lower energies the more recent data was 10-20% higher than the results of Stebbings et at (1960). The maximum in the cross-section was found to be at $\sim$ 12 eV, as before, but here $\sigma \simeq 1.8 \times 10^{-17}$ cm^2 instead of 1.4×10^{-17} cm^{-2}. No attempt was made by Cox and Smith to deduce the contribution from cascade effects.

2.2.2 Ionisation from the 2P and 2S states $H_o^* + e \rightarrow H_1^+ + 2e$

(a) 2P radiative state

Because of the short lifetime of the 2P state no experimental measurements of the ionisation cross-section have been made. However, several calculations have been performed, and the most reliable of these are shown in Figure 4. The full curve is based on the results of Mandl (1952), Omidvar (1965) and Prasad (1966) (the Born A approximation). These sets of calculations give essentially identical results.

The Born B approximation of Prasad (1966) gives better agreement with experiment for the case of 2S state ionisation, and this approximation applied to the 2P state is shown by crosses in Figure 4. It can be seen that the differences are not large in this case.

The calculations of Swan (1955) for 2P ionisation are in error by a factor of 2, and the numerical integrations performed do not appear to be very accurate (Omidvar, 1965).

(b) 2S metastable state

The cross-section for ionisation of the 2S metastable state has recently been measured by Dixon et al (1975), and the results are shown in Figure 5. The bars on the curve indicate the data range (using two different types of electron collector), not the error range. As noted above, the results are in reasonable agreement with the Born B approximation calculations carried out by Prasad (1966).

3. HYDROGEN MOLECULE REACTIONS

There is a range of reaction paths which an H_2 molecule can follow when bombarded by an electron. The threshold for a given reaction, the cross-section, and the shape of the cross-section curve depend upon the detailed collision mechanics and the internal state of the molecule. The various reaction paths have been discussed by Massey (1969, Chapter 13). Briefly, the thresholds for various processes lie in the order of dissociation into atoms, excitation, ionisation, dissociation to produce "slow" protons, and dissociation to produce "fast" protons.

3.1 Ionisation $H_2 + e \rightarrow H_2^+ + 2e$

Absolute cross-sections for this reaction have been directly determined by Rapp and Englander-Golden (1965). The cross-sections for electron energies in the range 16-1000 eV are given.

The results are shown in Figure 6, and are also presented in Kieffer and Dunn (1966). The data of Tate and Smith (1932), used to deduce the ionisation cross-section of atomic hydrogen (Section 2.1), agree well with the later data, except for small discrepancies around the maximum in the curve ($\simeq$ 4%), where the Tate and Smith values are slightly higher.

3.2 Dissociative ionisation $H_2 + e \rightarrow H_1^+ + H_o + 2e$

This reaction is thought to proceed via an excitation of the H_2 molecule followed by dissociation into a proton and an atom, which share 10-15 eV between them i.e.

$$H_2 + e \rightarrow (H_2)^* + e \rightarrow H_1^+ + H_o + 2e \quad .$$

The protons produced by this mechanism are therefore "fast" ions.

Cross-sections for this reaction have been measured by Rapp et al (1965) and are shown in Figure 7. The data are also presented in Kieffer and Dunn (1966). These results are for ions with kinetic energy greater than 2.5 eV. There are several uncertainties in the data i.e. an uncertain fraction of ions was collected, the method used to eliminate thermal ions may have also rejected some resulting from the dissociation, reflection of low energy ions from the collector could be a serious problem. However, these inaccuracies are not expected to alter the data greatly.

The energy distribution of the protons at an electron energy of 150 eV and a beam intersection angle $\theta = 305^{o}$ (the laboratory angle between the electron beam axis and the axis of the ion lens used to focus the protons produced before momentum selection and counting) is shown in Figure 8 (Kieffer and Dunn, 1967), and the distribution is shown for a range of electron energies in Figures 9 and 10. Here $\theta = 23^{o}$ (forward direction) and $\theta = 157^{o}$ (backward direction) results are shown. It can be seen that the protons have a range of energies of $\sim$ 4-14 eV, with mean energies of around 8-10 eV.

The experimental evidence indicated that most of the atomic ions came from the dissociative state 2 p σ_u of the H_2^+ molecular ion. However, discrepancies between experiment and theory (Figure 8) were present, and a number of possible explanations were considered. The most likely cause of the discrepancies was that repulsive high-lying Rydberg states of the H_2 molecule autoionise to form the observed H_1^+ with an apparent appearance potential consistent with the 2 pσ_u state of H_2^+ .

3.3 Dissociative excitation $H_2 + e \rightarrow H_o + H_o + e$

The cross-sections for this reaction have been measured by Corrigan (1965) and are shown in Fig. 11. The cross-section has essentially fallen to zero at energies of $\sim$ 80 eV. At the highest energies observed the measured apparent dissociation cross-section was closely equal to the measured ionisation cross-section of H_2. As dissociation into neutral atoms arises from the excitation of a triplet electronic state the true cross-section can be expected to fall rapidly with electron energy after passing through a maximum at an energy not far above the threshold. Corrigan subtracted the ionisation cross-section of H_2 from the measured apparent dissociation expected cross-section, and the resulting curve (Figure 11) has the form for singlet-triplet excitation.

There is no ambiguity in the interpretation of the results below the threshold for the production of H_2^+ (15.4 eV), but at higher electron energies problems arise because the method of detection of the H_o is rendered ambiguous. The neutral atoms were removed by Mo O_3 layers and the pressure fall in the apparatus was ascribed to dissociation. However, questions arise due to the possibilities of atoms making contact with surfaces other than the Mo O_3 and returning to the volume as molecules, and the Mo O_3 also acting as a clean-up agent for positive ions produced at the higher energies.

The reaction proceeds via an excited state of the neutral molecule i.e.

$$H_2 + e \rightarrow (H_2)^* + e \rightarrow H_o + H_o + e$$

and so the atoms produced have non-thermal velocities as they take away some of the dissociation energy. The energy distributions of the atoms have been investigated by Leventhal et al (1967). Some time-of-

flight results are shown in Fig. 12, for three values of the bombarding electron energy, and the deduced velocity distribution at one energy is shown in Fig. 13.

The distribution is seen, to consist of two groups of atoms with a "slow" peak becoming observable at 18 $\pm$ 2 eV and a "fast" peak appearing about 10.5 $\pm$ 2 eV higher. The velocity distribution shows maxima at (8.3 $\pm$ 0.5) and (31 $\pm$ 3) x 10^5 cm/sec, and the energy distribution shows maxima at 0.32 $\pm$ 0.05 eV and 4.7 $\pm$ 0.7 eV. The location of the two peaks did not change with increasing electron energy from $\sim$ 5 eV above threshold to 60 eV, but the relative intensity of the two peaks did vary markedly with energy, as seen from Fig. 12.

The slow atoms are thought to arise from excitation by electron bombardment to singly excited bound (attractive) states of the molecule lying just above the dissociation limit. On the other hand, because of the relatively higher threshold potential, the fast atoms are thought to arise from excitation to a doubly excited repulsive state of the molecule lying about 10 eV above the dissociation limit. As the electron energy is increased the excitation of the molecule to the higher energy state becomes more likely, and the number of fast atoms produced will increase.

4. H_2^+ ION REACTIONS

As in the case for H_2 reactions, there is a range of possible mechanisms for H_2^+ collisions with electrons, and these again depend on the electron energy and the initial state of the H_2^+ ion (Massey, 1969).

However, experiments with H_2^+ are complicated by the fact that it is not yet possible to prepare H_2^+ ions in a particular vibrational state, and measurements are generally made with the ions having a

distribution of vibrational energy.

H_2^+ ions are usually formed in an ion source by direct ionisation of ground state H_2. This process occurs within the Franck-Condon region of internuclear separation distances of the neutral molecule. Excited electronic states of H_2^+ are effectively repulsive, and therefore ionisation to any state of H_2^+ except the $1s\ \sigma_g$ ground state will result in subsequent dissociation. If the electrons which cause the ionisation in the source have energies > 18 eV, then all the vibrationally excited levels of the $1s\ \sigma_g$ state can be populated. Results of calculations for ionisation from the ground vibrational level of H_2 indicate that the fractional population of the H_2^+ levels is 0.09 for $\nu = 0$ (where ν is the vibrational quantum number), reaching a maximum of 0.18 at $\nu = 2$. The total for all levels with $\nu > 10$ is less than 0.05 (Dunn, 1966; Dance et al, 1967). The vibrational states are metastable in H_2^+, but the distribution may be modified by secondary collisions.

It is very difficult, therefore, to prepare H_2^+ ions in a particular state. As molecular H_2 is predominatly in the $\nu = 0$ state at room temperatures, the distribution of vibrational states should correspond to a distribution defined by the appropriate Franck-Condon factors. However, photodissociation measurements by von Busch and Dunn (1972) in a source designed to produce such a distribution found discrepancies between the measurements of the state population and theoretical predictions, although these differences were not large.

Because of the significant effect which the vibrational distribution can have upon reaction cross-sections, it is important to carry out measurements under realistic conditions i.e. conditions typical of an ion source discharge. Here the vibrational populations will be

perturbed from a pure Franck-Condon (or von Busch-Dunn) distribution, as the pressure in a source is generally high enough for secondary collisions to occur, and high energy electrons are used to give good ionisation efficienty. The source used by Peart and Dolder and Dunn and van Zyl (1967) did not represent this state of affairs very well, whereas the source used by Dance et al (1967) was much closer in conditions to these requirements.

4.1 Dissociative recombination $H_2^+ + e \rightarrow H_o + H_o$

The cross-section for this reaction has only recently been measured, using modulation techniques and crossed beam equipment, by Peart and Dolder (1974). The result is shown in Fig. 14, and it can be seen that this reaction has a large cross-section at low energies, but that the cross-section falls rapidly with increasing energy.

Previous data on this reaction were scarce. Bauer and Wu (1956) presented some calculations, although they disregarded molecular vibration and long-range Coulomb force effects. The onset energy was zero, and at this energy the σ_g transition is also zero but the σ_u transition cross-section was quoted as infinity. These correspond to the cases where the incident electron is inclined and parallel to the nuclear axis, respectively. The values of $(\sigma_g + \sigma_u)$ are in order-of-magnitude agreement with experiments at lower energies but are an order of magnitude too high at $\sim$ 1 eV, and increase rather than decrease with increasing energy.

The reaction is thought to be a two-stage process proceeding via electron capture to give a hydrogen molecule in an unstable excited state, which then dissociates i.e.

$$H_2^+ + e \rightarrow (H_2)^* \rightarrow H_o + H_o \quad .$$

The atoms produced are therefore non-thermal, taking away some of the dissociation energy. Energy distributions have not been measured for this reaction, but if the excited state is the lowest triplet state of the molecule, which is a repulsive state, dissociation into neutral atoms with $\sim$ 2.2 eV kinetic energy is to be expected.

4.2 Dissociative excitation $H_2^+ + e \rightarrow H_1^+ + H_o + e$

Dissociation of the H_2^+ ion via an excited state is thought to take place via two routes (Dunn and van Zyl, 1967)

$$H_2^+ (1s\,\sigma_g) + e \rightarrow H_2^+ (2p\sigma_u) + e \rightarrow H_1^+ + H_o + e$$

$$H_2^+ (1s\,\sigma_g) + e \rightarrow H_2^+ (2p\pi_u,\ 2s\sigma_g,\ \text{others}) \rightarrow H_1^+ + H_o^* + e\ .$$

Until recently the only determinations of this cross-section have been theoretical ones e.g. Ivash (1958), Peek (1964). However, absolute values, measured by Peart and Dolder (1972a) using modulation techniques and crossed beams, are now available.

The results are shown by the solid line in Figure 15. As a comparison with theory it was assumed that the cross-section was given by the sum of the $1s\sigma_g \rightarrow 2p\sigma_u$ and $1s\sigma_g \rightarrow 2p\pi_u$ cross-sections, with states other than these making negligible contributions to the excitation, and averaging these cross-sections over the vibrational states of H_2^+. Agreement with theory was good, down to the lowest energy at which data were taken (25.4 eV). The dashed portion of the curve in Fig. 15 is based on the behaviour of the theoretical solution of Peek (1964) to give an indication of the low-energy behaviour.

4.3 Dissociative ionisation $H_2^+ + e \rightarrow H_1^+ + H_1^+ + 2e$

This reaction does not proceed via an excited state of the H_2^+ ion, as in dissociative excitation, but splits directly into two protons. The threshold for the reaction is larger than the vibrational

or rotational energies, and so the cross-sections are unlikely to be very sensitive to the initial molecular ion excitation state.

The cross-section for the reaction, taken from the tabular results of Peart and Dolder (1973), are shown in Fig. 16.

4.4 Total proton production $H_2^+ + e \rightarrow$ protons

Until the recent measurements of the different reactions which contribute to the proton production from H_2^+ (sections 4.2 and 4.3) only the cross-section for total proton production by electron bombardment had been measured. Peart and Dolder (1971, 1972b) measured the sum of the dissociative excitation and ionisation cross-sections i.e. $\sigma_p^1 = \sigma_e + \sigma_i$. Dunn and van Zyl (1967) and Dance et al (1967) measured $\sigma_p = \sigma_e + 2\sigma_i$.

As the value of σ_i is small compared to σ_e the different sets of results should agree fairly well. They do in the case of Peart and Dolder and Dunn and van Zyl, where the difference is very close to calculated σ_i values (although the errors are expected to be large for small differences). However, the Dance et al results are too low at energies $\lesssim$ 100 eV. This is thought to be due to the type of source used, in which the plasma could easily destroy the highly excited states of H_2^+, so that the vibrational populations in the beams would be weighted towards the lower states which have smaller cross-sections. As noted above, these conditions are thought to be more respresentative of those existing in high current ion source discharges.

The results of Peart and Dolder (1971, 1972b) are shown in Fig.17. Below about 12 eV the proton production is via vibrationally excited stated of the H_2^+ ion. The results of Dance et al (1967) are also given, and the difference in the data can be clearly seen.

Also shown in Fig. 17 are the results of calculations for the proton production cross-section derived by summing the excitation cross-sections over the relevant Franck-Condon factors and allowing for the contribution from dissociative ionisation, as explained in Dance et al (1967). Good agreement with experiment is found.

5. H_3^+ ION REACTIONS

5.1 H_3^+ ion formation $H_2^+ + H_2 \rightarrow H_3^+ + H_o$

Recent studies of the mechanism for this reaction (Lees and Rol, 1974) have shown that hydrogen atom transfer is the dominant mechanism at interaction energies above ≃ 6-7 eV, but below this energy both proton transfer and hydrogen atom transfer contribute nearly equally to the reaction.

The cross-section for the reaction has been measured in swarm experiments by Giese and Maier (1963) and by the use of merged-beam techniques by Neynaber and Trujillo (1968). The results agreed within experimental error. In the latter work, cross-section determinations at various interaction energies were accompanied by measurements at 1 eV, so that a ratio was obtained. An absolute value of the cross-section at 1 eV was found, although its estimated error was considerably larger than errors associated with the cross-section ratios. The value was

$$\sigma_{1\ eV} = 1.2 \times 10^{-15}\ ^{+\ 37\%}_{-\ 26\%}\ cm^2 \ .$$

Values of the cross-section measured by Neynaber and Trujillo are shown in Figure 18, with the error at 1 eV denoted by the bar.

5.2 Dissociative recombination $H_3^+ + e \rightarrow$ neutral H_o

In the case of H_2^+, neutral atoms can be produced via dissociative recombination or dissociative excitation i.e.

$$H_2^+ + e \rightarrow H_o + H_o$$

$$\rightarrow H_o + H_1^+ + e \quad .$$

In the case of H_3^+ the situation is more complicated, in that one, two or three hydrogen atoms can be formed according to the way the H_3^+ ion breaks up i.e.

$$H_3^+ + e \rightarrow H_o + H_o + H_o$$

$$\rightarrow H_o + H_2$$

$$\rightarrow H_o + H_o + H_1^+ + e \quad .$$

The dissociative recombination cross-sections have been measured by Peart and Dolder (1974c), using pulse height discrimination methods and inclined beams. The pulses due to the atoms from the dissociative excitation mechanism could be rejected using this technique. The results are shown in Fig. 19, and it can be seen that the cross-section is very similar to that for the dissociative recombination reaction in H_2^+ (Fig. 14).

Measurements at thermal energies, by Leu et al (1973), of the recombination coefficients can be converted to cross-sections, and extrapolation of the Peart and Dolder results to lower energies passes very close to these values.

The higher energy measurements were made using H_3^+ which had been de-excited to a state with negligible internal energy, possibly via the reaction

$$(H_3^+)^* + H_2 \rightarrow (H_2)^* + H_3^+$$

i.e. a high-pressure mechanism. The presence of electronically excited H_3^+ states is expected to modify the cross-sections.

5.3 Dissociative excitation $H_3^+ + e \rightarrow H_o + H_o + H_1^+ + e$

The cross-section for proton production via dissociative excitation can be measured for low electron energies, and the results of Peart and Dolder (1974b) are shown in Fig. 20. The values are similar to those for H_2^+ at low energies. The measurements were carried out using de-excited H_3^+ ions, and it was estimated that about four collisions with neutral H_2 molecules were required to give de-excited ions.

If the cross-section measurements for proton production are extended to higher energies (Peart and Dolder, 1975) then a rapid increase in the cross-section is found between 20 and 30 eV. This is attributed to the existance of several unstable states of H_3^+ with energies about 20 eV above the ground state (Kawaoka and Borkman, 1971), with dissociation of these states proceeding via the reactions

$$H_3^+ + e \rightarrow H_o + H_o + H_1^+ + e$$
$$\rightarrow H_2 + H_1^+ + e$$
$$\rightarrow H_2^+ + H_o + e \quad .$$

The dissociative excitation mechanism can be regarded as occurring from the ground state of H_3^+, with contributions from higher states occurring at higher electron energies.

This situation at higher energies can be compared with that for the case of H_2^+ a few years ago, when the only measurements available were those of the cross-section for total proton production (Section 4.4) and data on the reactions which contribute to this production (Sections 4.2 and 4.3) were not yet available.

REACTION	ONSET ENERGY (eV)	σ_{max} (cm^2)	E at σ_{max} (eV)	REFERENCE
$H_o + e \rightarrow H_1^+ + 2e$	13.5	7×10^{-17}	64	Fite and Brackman (1958a)
$H_o + e \rightarrow H_o^* + e$ 2P	10.2	7.4×10^{-17}	50	Fite and Brackman (1958b)
2S	10.15	1.4×10^{-17}	12	Stebbings et al (1960)
$H_o^* + e \rightarrow H_1^+ + 2e$ 2P	3.3	1.7×10^{-15}	9	Omidvar (1965); Prasad (1966)
2S	3.3	9.4×10^{-16}	13	Dixon et al (1975)
$H_2 + e \rightarrow H_2^+ + 2e$	15.4	9.8×10^{-17}	70	Rapp and Englander-Golden (1965)
$H_2 + e \rightarrow H_1^+ + H_o + 2e$	18.0	5.8×10^{-18}	100	Rapp et al (1965)
$H_2 + e \rightarrow H_o + H_o + e$	8.8	9×10^{-17}	17	Corrigan (1965)
$H_2^+ + e \rightarrow H_1^+ + H_o + e$	12.4	4.3×10^{-16}	~24	Peart and Dolder (1972a)
$H_2^+ + e \rightarrow H_1^+ + H_1^+ + 2e$	17	1.75×10^{-17}	105	Peart and Dolder (1973)
$H_2^+ + e \rightarrow H_o + H_o$	Thermal	Large ($\sim 10^{-14}$)	0	Peart and Dolder (1974a)
$H_2^+ + H_2 \rightarrow H_3^+ + H_o$	Thermal	Large ($\sim 10^{-14}$)	0	Neynaber and Trujillo (1968)
$H_3^+ + e \rightarrow$ neutral H_o	Thermal	Large ($\sim 10^{-14}$)	0	Peart and Dolder (1974c)
$H_3^+ + e \rightarrow H_1^+ + H_o + H_o + e$	15	3.5×10^{-16}	17	Peart and Dolder (1974b)

REFERENCES

BARNETT, C.F. et al (1964), ORNL - 3113 (Rev).

BAUER, E. and WU, T.Y. (1956), Can. J. Phys., 34, 1436.

CORRIGAN, S.J.B. (1965), J. Chem. Phys., 43, 4381.

COX, D.M. and SMITH, S.J. (1971), VIIth, ICPEAC, Amsterdam.

DANCE, D.F. et al (1967), Proc. Phys. Soc., 92, 577.

DIXON, A.J., VON ENGEL, A. and HARRISON, M.F.A. (1975), Proc. Roy. Soc., A343, 333.

DUNN, G.H. (1966), J. Chem. Phys., 44, 2592.

DUNN, G.H. and VAN ZYL, B. (1967), Phys. Rev., 154, 40.

FITE, W.L. and BRACKMAN, R.T. (1958a), Phys. Rev., 112, 1141.

FITE, W.L. and BRACKMAN, R.T. (1958b), Phys. Rev., 112, 1151.

FITE, W.L. et al (1959), Phys. Rev., 116, 363.

FREEMAN, R.L. and JONES, E.M. (1974), Culham Lab. Rpt. CLM-R137.

GIESE, C.F. and MAIER, W.B. II (1963), J. Chem. Phys., 39, 739.

GREEN, T.S. (1974), Rep. Prog. Phys., 37, 1257.

GREEN, T.S. et al (1975), Paper 93, 7th European Conf. on Controlled Fusion and Plasma Physics, Lausanne.

HILS, D. et al (1966), Proc. Phys. Soc., 89, 35.

IVASH, E.V. (1958), Phys. Rev., 112, 155.

KAWAOKA, K. and BORKMAN, R.F. (1971), J. Chem. Phys., 54, 4234.

KIEFFER, L.J. and DUNN, G.H. (1966), Rev. Mod. Phys., 38, 1.

KIEFFER, L.J. and DUNN, G.H. (1967), Phys. Rev., 158, 61.

LEES, A.B. and ROL, P.K. (1974), J. Chem. Phys., 61, 4444.

LEU, M.T., BIONDI, M.A. and JOHNSEN, R. (1973), Phys. Rev., A8, 413.

LEVENTHAL, M., ROBISCOE, R.T. and LEA, K.R. (1967), Phys. Rev., 158, 49.

LICHTEN, W. (1961), Phys. Rev. Lett., 6, 12.

LONG, R.L., COX, D.M. and SMITH, S.J. (1968), J. Res. Nat. Bur. Stand., 72A, 521.

MANDL, F. (1952), AERE T/R 1006.

MARTIN, A.R. and GREEN, T.S. (1976), to be published.

MASSEY, H.S.W. (1969), Electronic and Ionic Impact Phenomena, Vol.II, Clarendon Press.

NEYNABER, R.H. and TRUJILLO, S.M. (1968), Phys. Rev. 167, 63.

OMIDVAR, K. (1965), Phys. Rev., 140, A26.

PEART, B. and DOLDER, K.T. (1971), J. Phys. B., 4, 1496.

(1972a), J. Phys. B., 5, 860.

(1972b), J. Phys. B., 5, 1554.

(1974a), J. Phys. B., 7, 236.

(1974b), J. Phys. B., 7, 1567.

(1974c), J. Phys. B., 7, 1948.

(1975), J. Phys. B., 8, L143.

PEAK, J.M. (1964), Phys. Rev., 134, A877.

PRASAD, S.S. (1966), Proc. Phys. Soc., 87, 393.

RAPP, D. and ENGLANDER-GOLDEN, P. (1965), J. Chem. Phys., 43, 1464.

RAPP, D., ENGLANDER-GOLDEN, P. and BRIGLIA, D.D. (1965), J.Chem. Phys., 42, 4081.

STEBBINGS, R.F. et al (1960), Phys. Rev., 119, 1939.

SWAN, P. (1955), Proc. Phys. Soc., 68A, 1157.

TATE, J.T. and SMITH, P.T. (1932), Phys. Rev., 39, 270.

VAN BRUNT, R.J. and KIEFFER, L.J. (1970), Phys. Rev., 2A, 1293.

VON BUSCH, F. and DUNN, G.H. (1972), Phys. Rev., 5A, 1726.

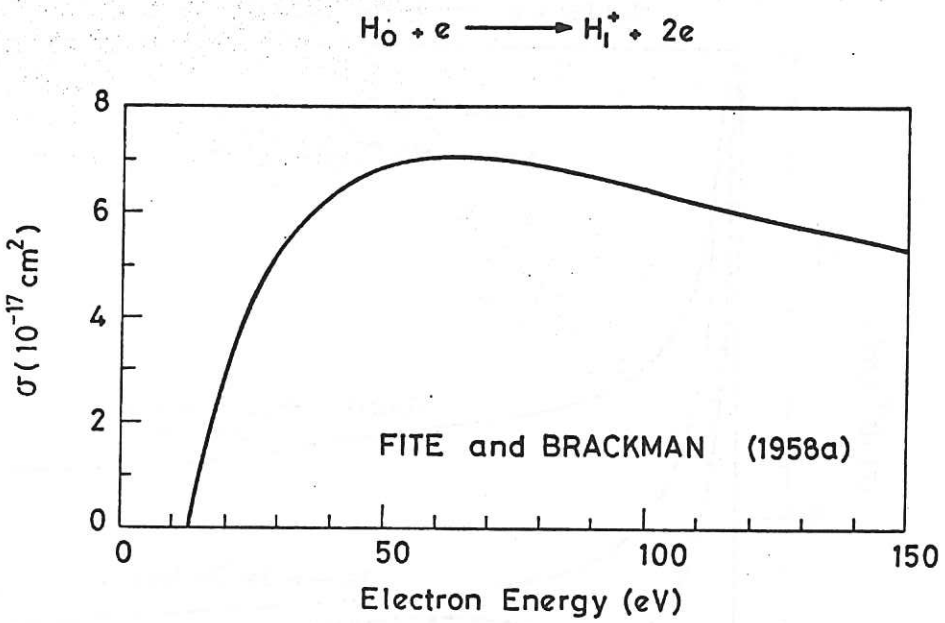

Fig. 1 Atomic hydrogen ionisation cross-section

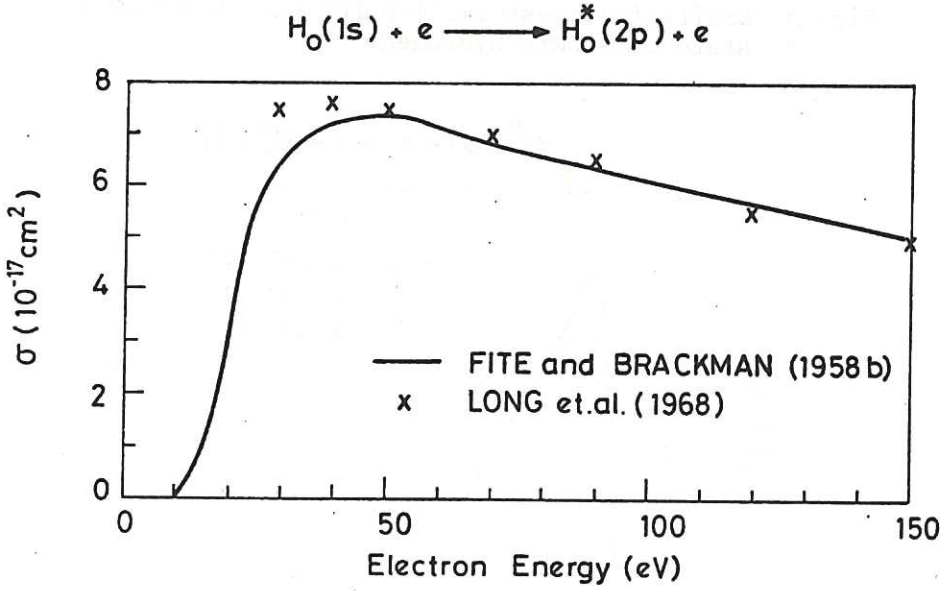

Fig. 2 Excitation cross-section for the 2P radiative state of atomic hydrogen.

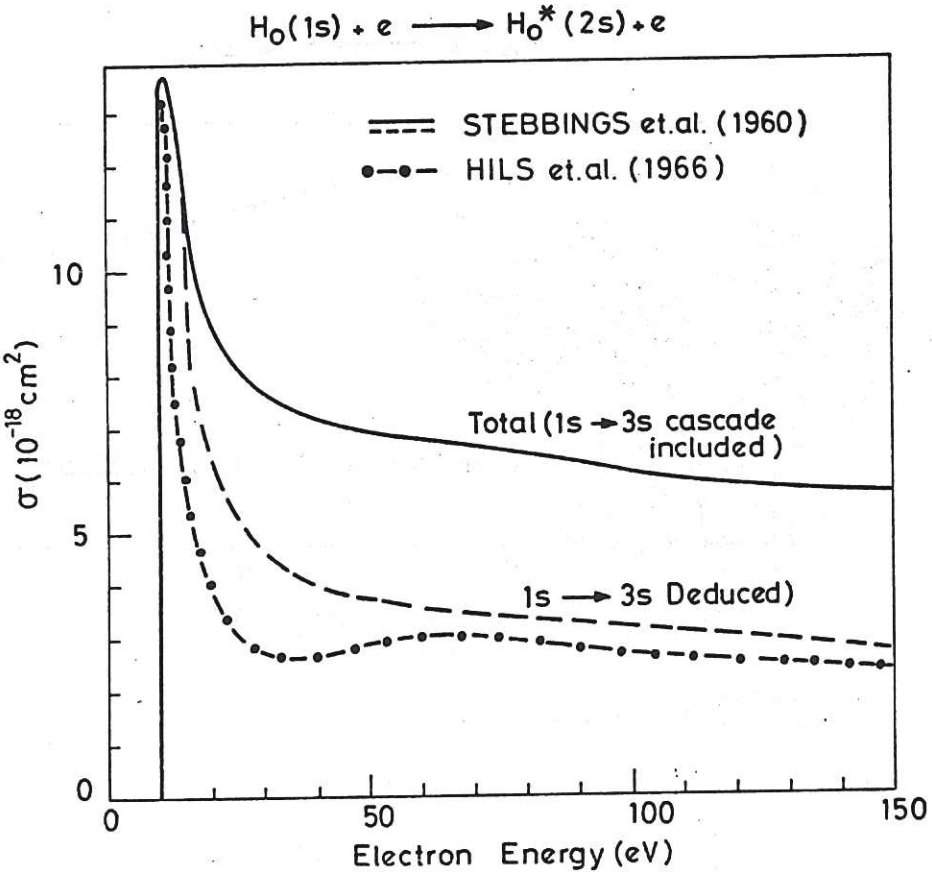

Fig. 3 Excitation cross-section for the 2S metastable state of atomic hydrogen.

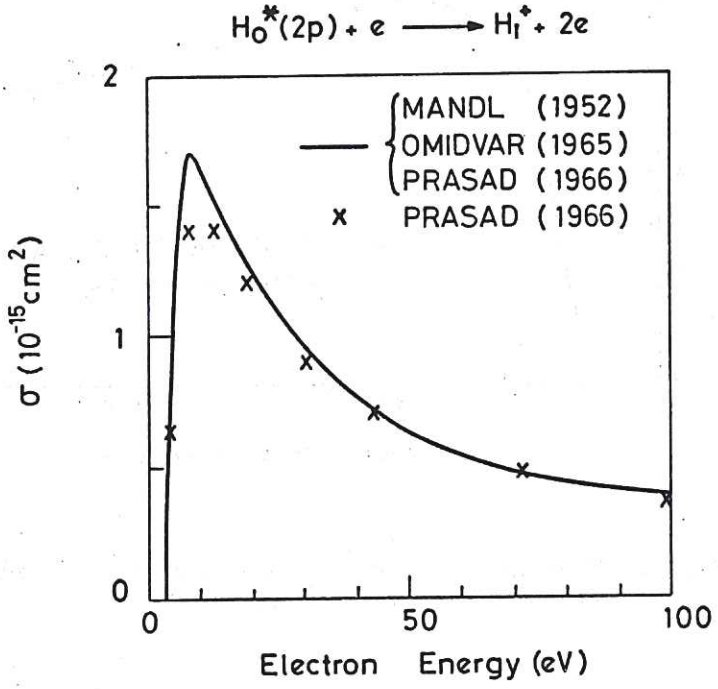

Fig. 4 Ionisation cross-section of the 2P state.

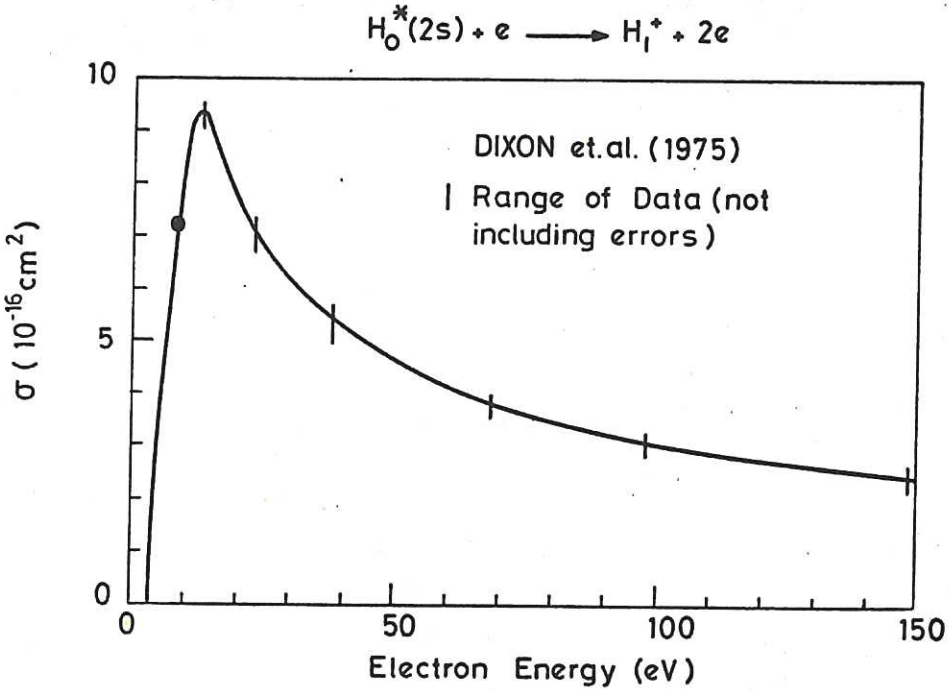

Fig. 5 Ionisation cross-section of the 2S state.

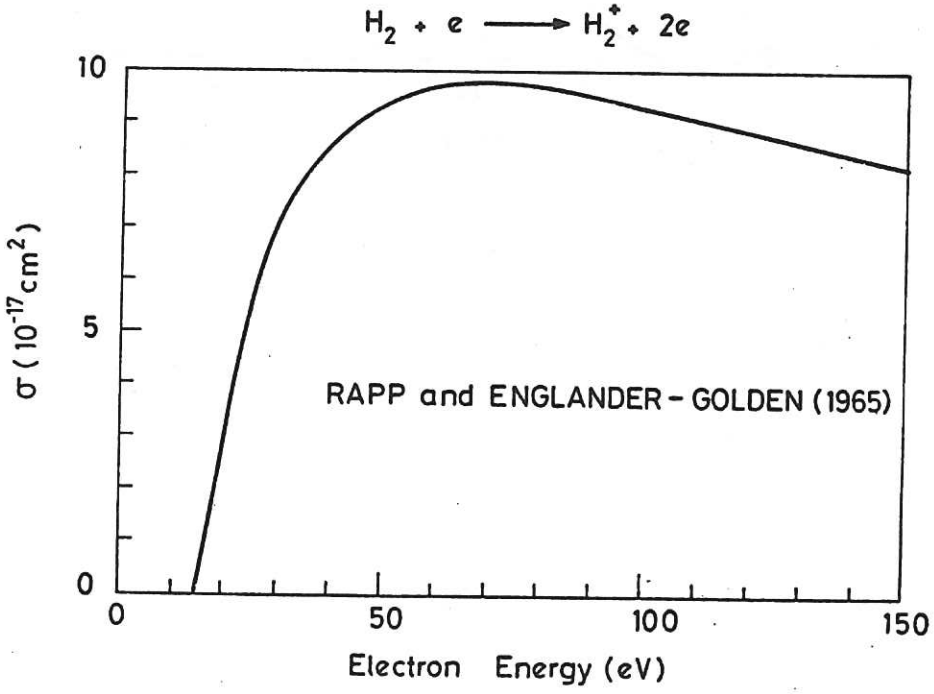

Fig. 6 Molecular hydrogen ionisation cross-section.

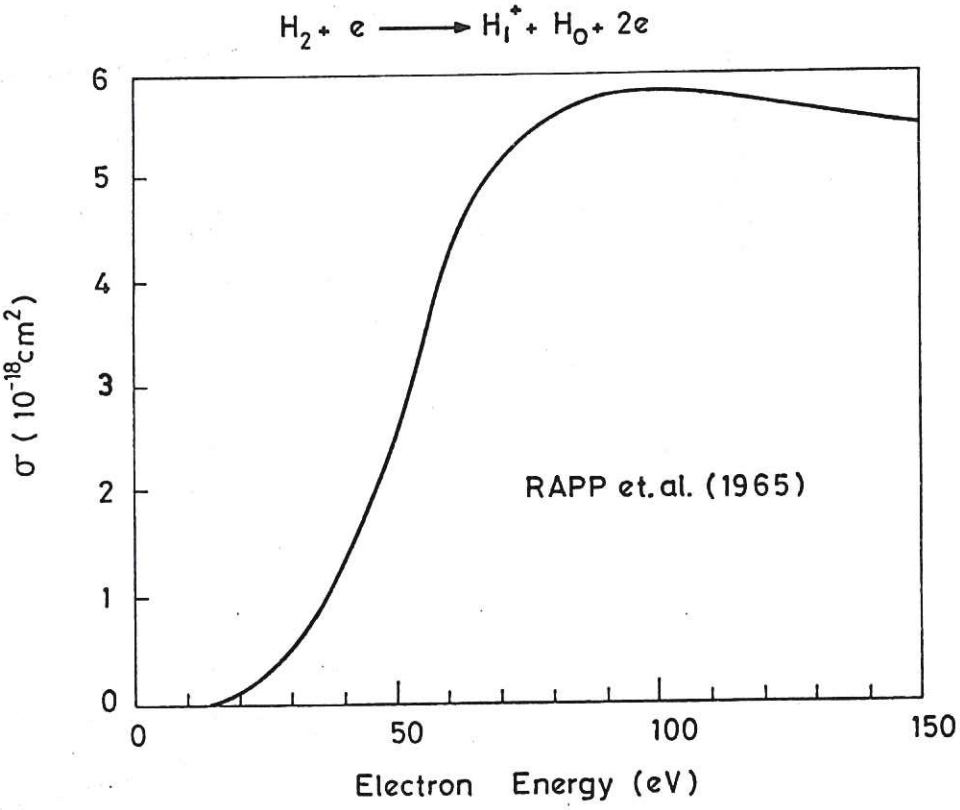

Fig. 7 Dissociative ionisation cross-section for molecular hydrogen.

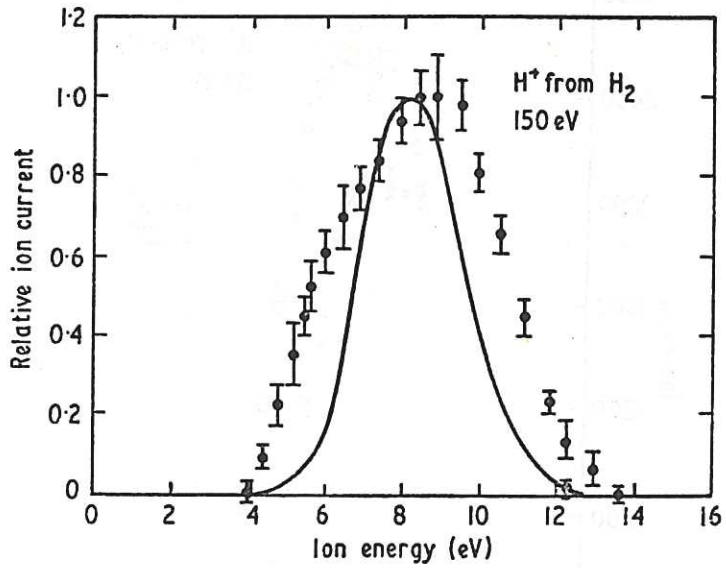

Fig. 8 Relative numbers of H_1^+ ions versus ion energy; observed values - dots, Franck-Condon predictions - solid line.

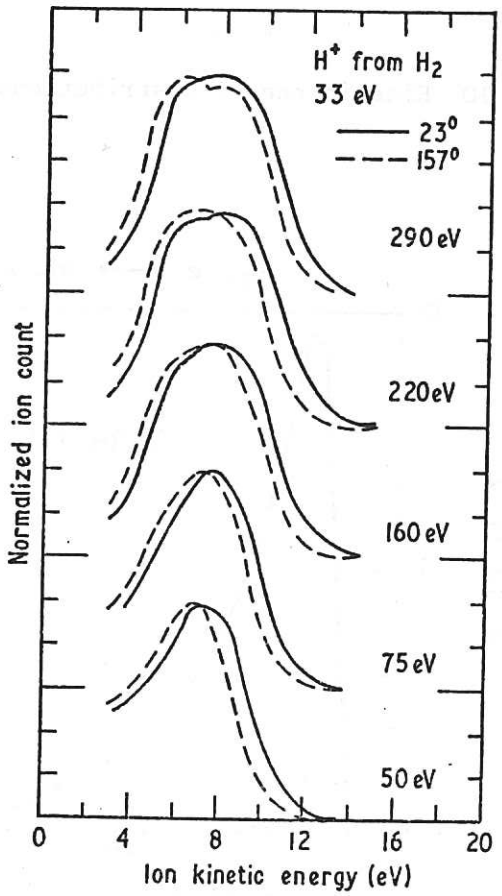

Fig. 9 Observed kinetic-energy distributions of H_1^+, for a range of electron energies.

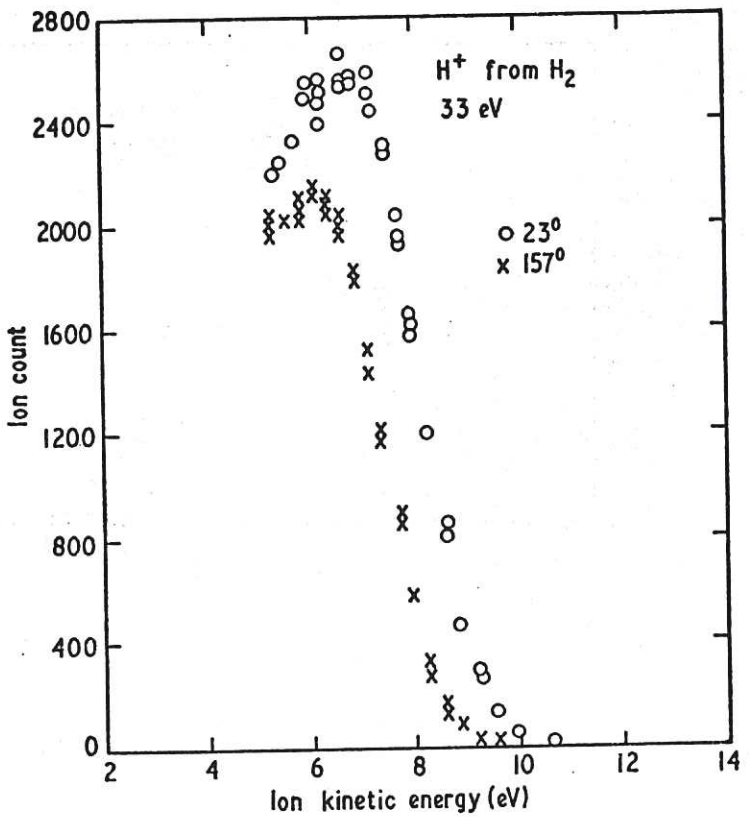

Fig. 10 Kinetic energy distributions of H_1^+

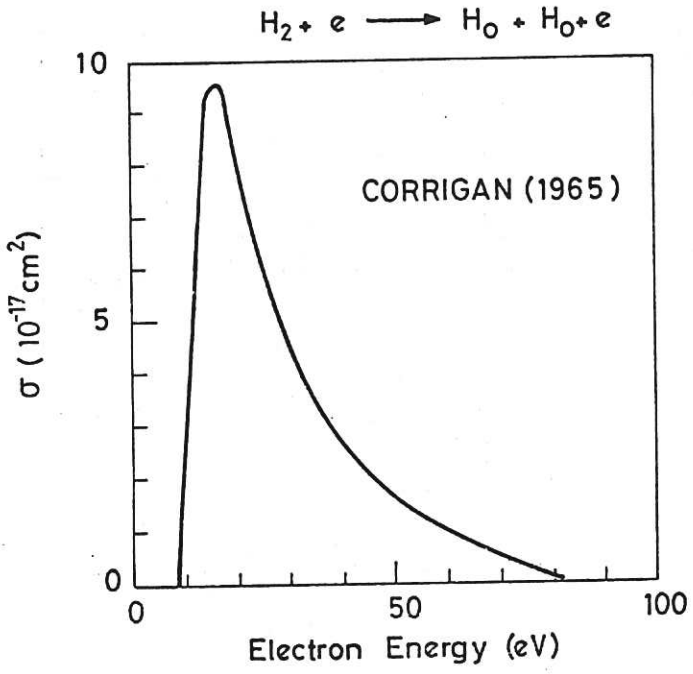

Fig. 11 Dissociative excitation cross-section for molecular hydrogen.

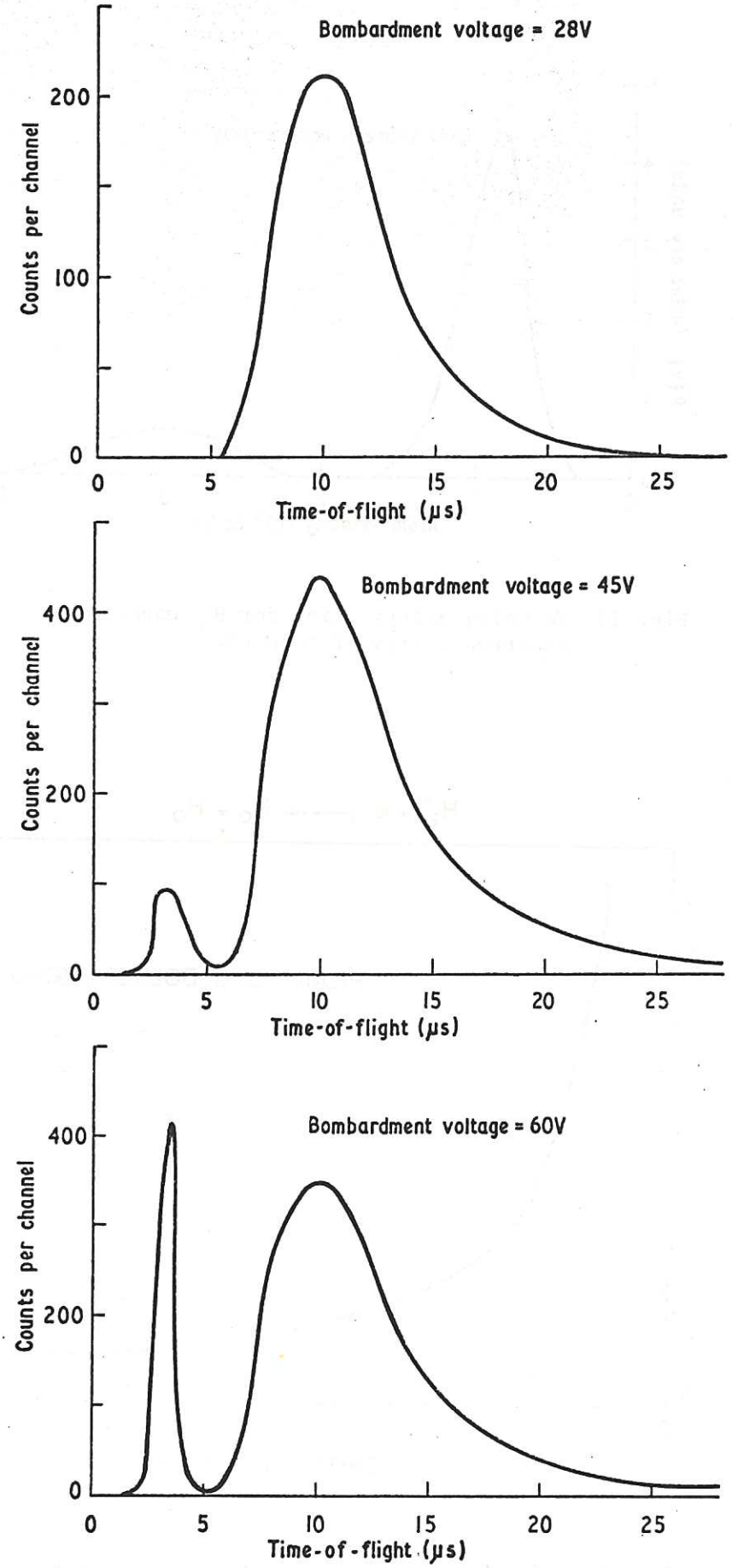

Fig. 12 Time-of-flight spectra for H_o atoms at several electron bombardment voltages.

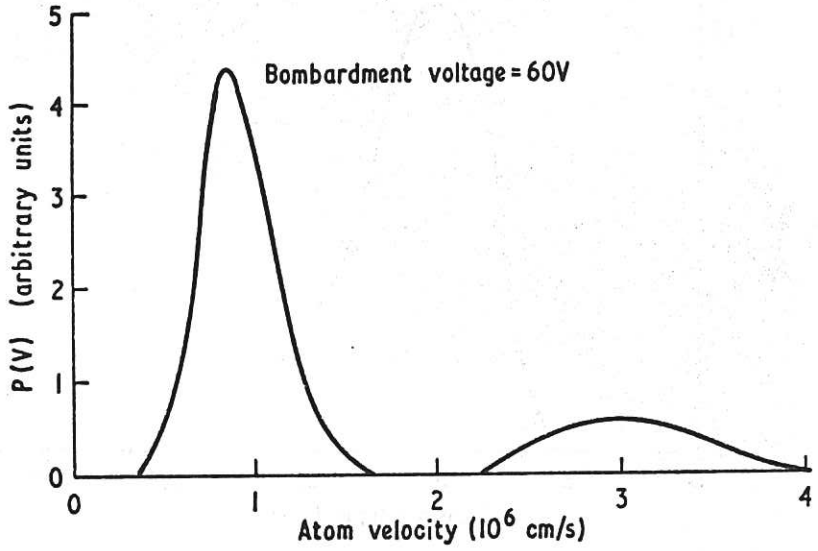

Fig. 13 Velocity distribution for H_o atoms at an electron energy of ∿ 60 eV.

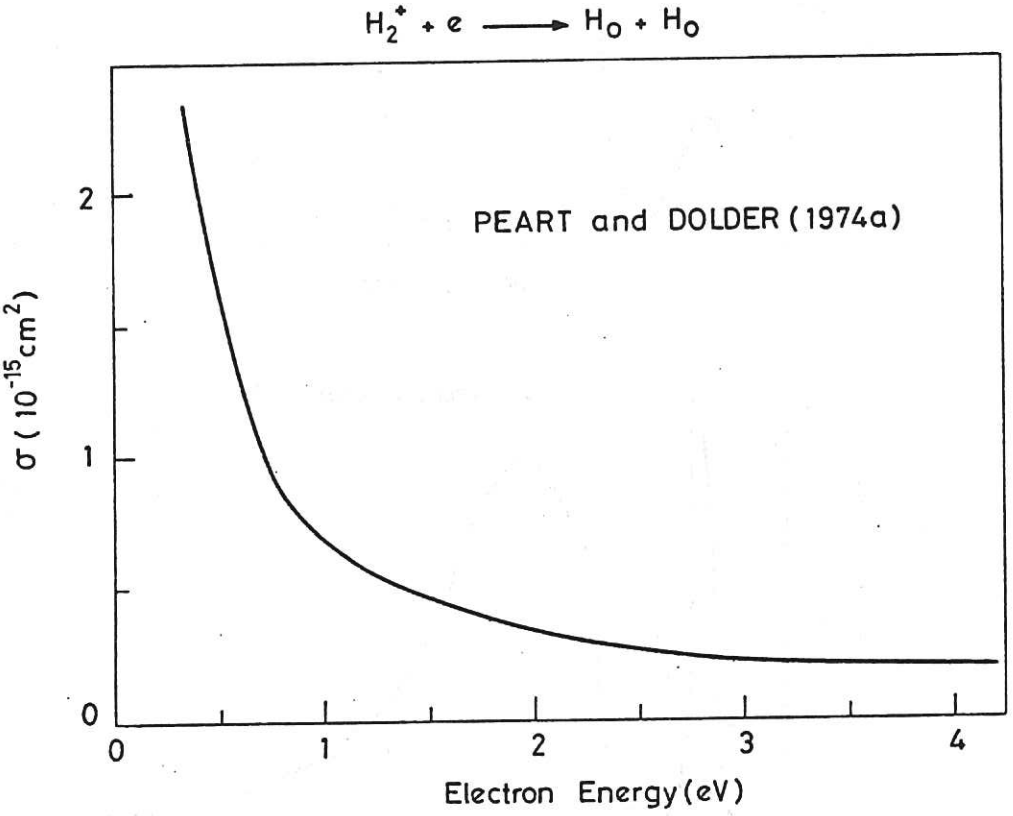

Fig. 14 Dissociative recombination cross-section of H_2^+.

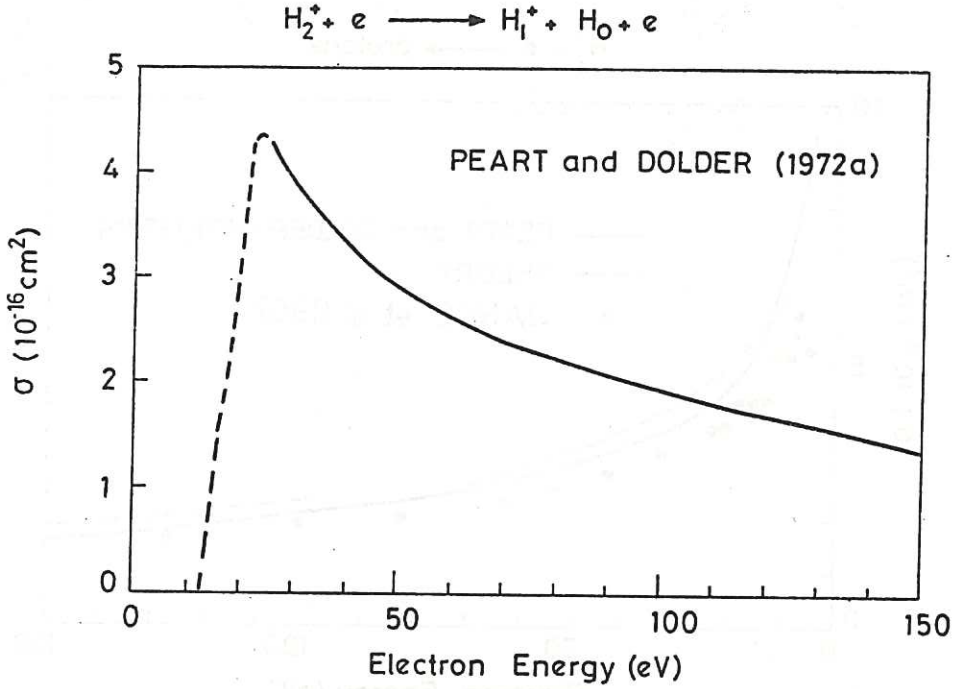

Fig. 15 Dissociative excitation cross-section of H_2^+ .

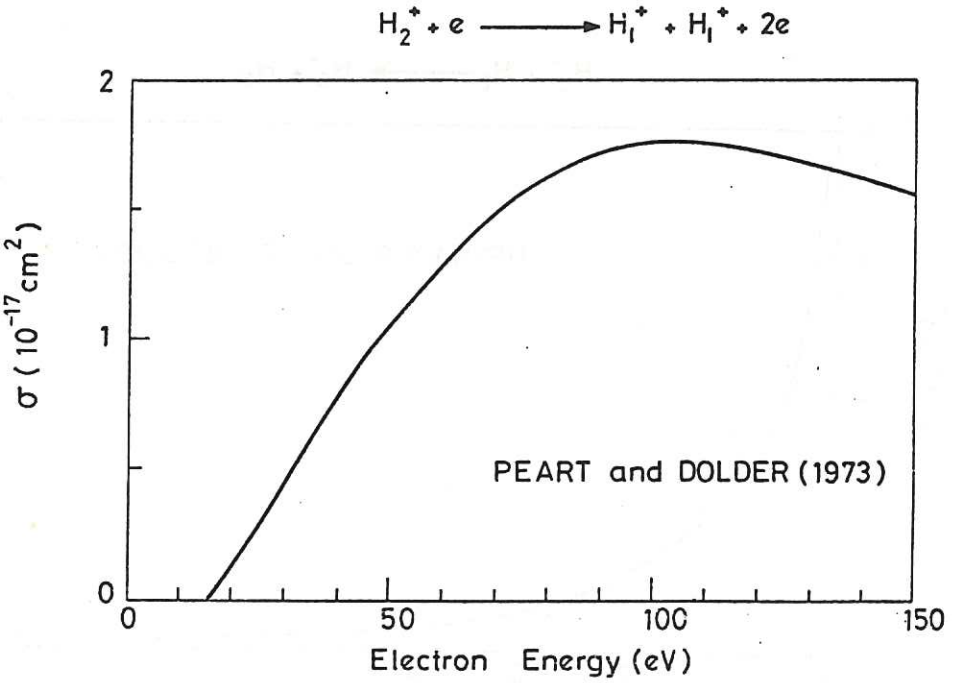

Fig. 16 Dissociative ionisation cross-section of H_2^+ .

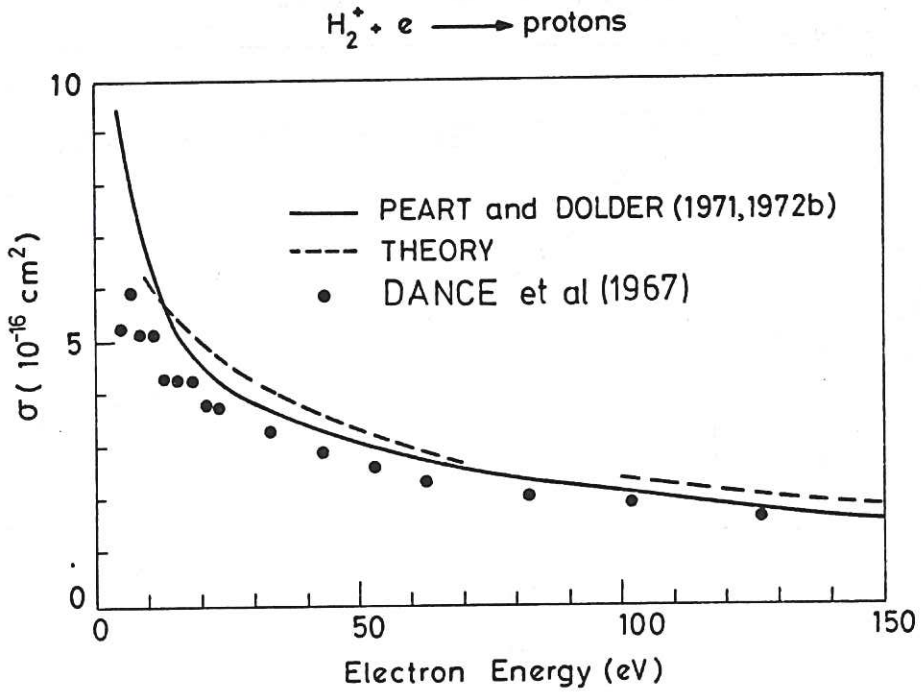

Fig. 17 Total proton production cross-section for electrons bombarding H_2^+ ions.

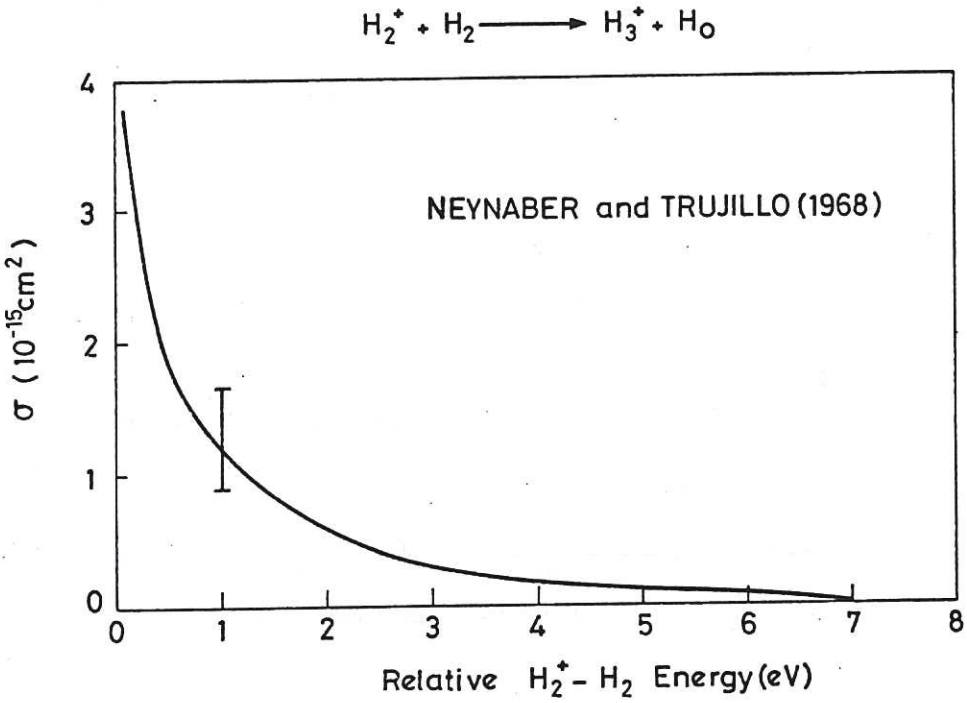

Fig. 18 H_3^+ ion formation cross-section.

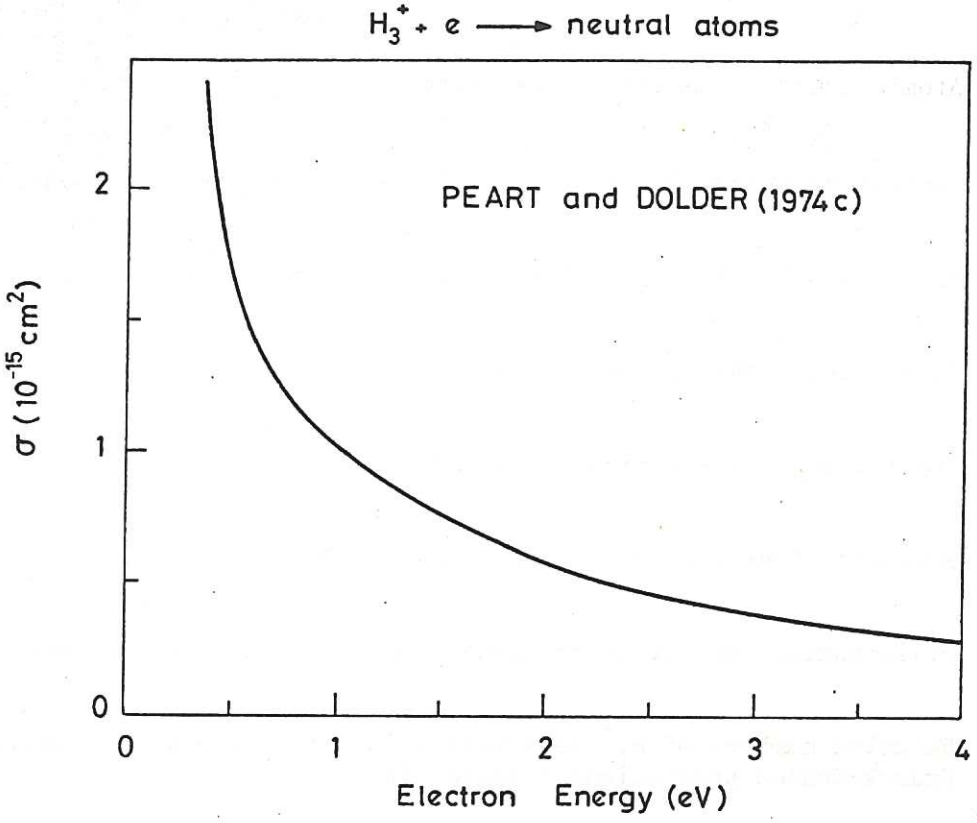

Fig. 19 Dissociative recombination cross-section of H_3^+.

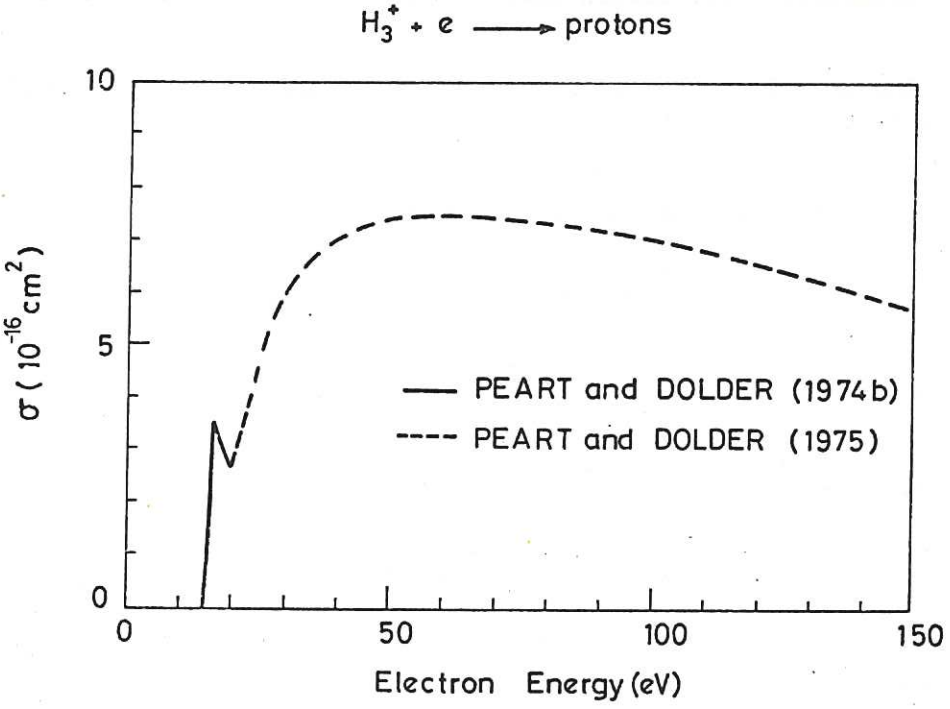

Fig. 20 Dissociative excitation cross-section of H_3^+.

Fig. 1. Atomic hydrogen ionisation cross-section

Fig. 2. Excitation cross-section for the 2P radiative state of atomic hydrogen.

Fig. 3. Excitation cross-section for the 2S metastable state of atomic hydrogen.

Fig. 4. Ionisation cross-section of the 2P state.

Fig. 5. Ionisation cross-section of the 2S state.

Fig. 6. Molecular hydrogen ionisation cross-section.

Fig. 7. Dissociative ionisation cross-section for molecular hydrogen.

Fig. 8. Relative numbers of H_1^+ ions versus ion energy; observed values - dots, Franck-Condon predictions - solid line.

Fig. 9. Observed kinetic-energy distributions of H_1^+, for a range of electron energies.

Fig. 10. Kinetic energy distributions of H_1^+.

Fig. 11. Dissociative excitation cross-section for molecular hydrogen.

Fig. 12. Time-of-flight spectra for H_o atoms at several electron bombardment voltages.

Fig. 13. Velocity distribution for H_o atoms at an electron energy of $\sim$ 60 eV.

Fig. 14. Dissociative recombination cross-section of H_2^+.

Fig. 15. Dissociative excitation cross-section of H_2^+.

Fig. 16. Dissociative ionisation cross-section of H_2^+.

Fig. 17. Total proton production cross-section for electrons bombarding H_2^+ ions.

Fig. 18. H_3^+ ion formation cross-section.

Fig. 19. Dissociative recombination cross-section of H_3^+.

Fig. 20. Dissociative excitation cross-section of H_3^+.

HER MAJESTY'S STATIONERY OFFICE

Government Bookshops

49 High Holborn, London WC1V 6HB
13a Castle Street, Edinburgh EH2 3AR
41 The Hayes, Cardiff CF1 1JW
Brazennose Street, Manchester M60 8AS
Wine Street, Bristol BS1 2BQ
258 Broad Street, Birmingham B1 2HE
80 Chichester Street, Belfast BT1 4JY

Government publications are also available through booksellers